Reliability Evaluation of a 1.85 mm Blind Mating Coaxial Interconnect for mmWave ATE Applications

António José Rodrigues Mendes
antonio.rodrigues.mendes@tecnico.ulisboa.pt
Instituto Superior Técnico, Universidade de Lisboa, Portugal

January 2020

Abstract

Over the past years, the transmission of extensive volumes of data in Integrated Circuits (ICs) have been a challenge of telecommunication and networking areas. The emergence of 5G and the wireless gigabit (WiGig) technology, require an operating frequency range between 24 and 70GHz with further increase in the future. IC testing is performed by Automatic Test Equipment (ATE) integrated in a semiconductor test cell. The interconnection in an ATE, between the Device Under Test (DUT) and the Printed Circuit Board (PCB) test fixture, is established by a custom designed 1.85 mm blind mating coaxial connector. Therefore, this work focus on the reliability evaluation of this connector. The connectors evaluation was based in several electrical, mechanical and dimensional measurements along a cyclic testing (60,000 cycles) performed in an ATE system. Moreover, a failure mode and effects analysis (FMEA) was achieved by using techniques such as the Scanning Electron Microscope (SEM) and Computed Tomography (CT). Furthermore, a mechanical simulation between of pin and socket contact during docking, was conducted based on the Finite Element Method (FEM). From a total of 14 tested connectors: 10 to measure S-parameters, 2 to measure contact resistance and other 2 to measure S-parameters after an accelerated test (ACT), 11 have failed. The failure occurred at the female pair, specifically at the socket keyhole. Fatigue is the failure mechanism responsible for the cracking. Overall, the 1.85 mm blind mating coaxial connector presented a high reliability (over 40,000 cycles) for ATE applications.
Keywords: 5G, IC testing, ATE, 1.85 blind mating coaxial connector, reliability evaluation

1. Introduction

The developments of the new 5G wireless communication technology brings new challenges concerning IC testing. The back-end stage of the semiconductor manufacturing process, where ATE is used, is divided in IC testing before packaging (wafer testing) and after packaging (package testing). Both require a reliable connection between the ATE PCB test fixture and the DUT. Figure 1 shows an ATE test cell for package testing [15, 7].

Figure 1: ATE test cell for DDR testing with an ATE system and a robotic handler that inserts the packaged IC into the ATE.

This interconnection can be performed by blind mating coaxial connectors. Considering that the frequencies for testing 5G-NR (New Radio) require 24, 28 and 39 GHz and for wireless gigabit (WiGig) devices a frequency from 56 GHz to 70 GHz, then for mmwave wireless applications one connector that fulfills this range is the 1.85 mm. The use of blind mating coaxial connectors to establish a connection between the ATE system and the DUT PCB test fixture which connects the DUT during the test of an IC, requires not only the need of electrical performance but also reliability (multiple dock and undocking cycles). The 1.85 mm blind mating coaxial connector (designed by Signal Microwave for Advantest) is used on the Advantest V93000 wavescale milimeter cardcage ATE system [12, 3, 1, 13].

The goal of this work was to study the maximum number of cycles the connector withstands while the electrical requirements are still compliant. To do that, a reliability evaluation plan was developed where several electrical, mechanical and dimensional measurements are performed as well as a failure analysis on the connector using SEM and CT scan. Moreover, the number of cycles before

failure for an ATE system is calculated based on 10 connectors (tested under the same conditions) using statistical distributions models. Finally, based on the FEM, a mechanical simulation is performed as an alternative method to study the reliability of the connector.

2. Background

2.1. Standards

MIL-PRF-39012 and IEEE 287 (subcommittee on precision coaxial connectors) are the more important standards for coaxial connectors[11, 10]. IEEE 287 standard addresses test methods and concepts around the connector technology with detailed specifications (Table 1) for each connector in terms of electrical, mechanical and environment conditions [22]. A limitation of this standard is that it is only applied to connectors with a threaded nut design. MIL-PRF-39012 describes the materials and manufacturing methods used for the centre contacts (pin and socket), connector housing and spring members, i.e. requires that the gold thickness of centre contacts has a minimum of 1.27 μm [16].

Electrical Specifications	
Cutoff Frequency	73.3 GHz
Contact Resistance	0.15 mΩ
Mechanical Specifications	
Connect/Disconnect Life	5,000 cycles
Maximum Insertion Force	0.9 N
Minimum Withdrawal Force	0.14 N
Environmental Specifications	
Temperature	13-33 ^{o}C
Humidity	20-80 % RH

Table 1: Electrical, mechanical and environmental specifications for 1.85 mm coaxial connector.

Another standards, like MIL 348, MIL 202G, IPC-9592 and MIL-HDBK-217, describe inspection and durability test methods and its reliability for testing the connectors. The IPC-9592 standard makes reference to the JESD22-A101, which is a standard that defines a reliability evaluation of non-hermetic packaged solid-state devices in humid environments. The conditions of this test are 85 ^{o}C and 85 % humidity during 72 hours. This is an example of a high temperature/ high humidity accelerated test usually performed in the aerospace industry [25]. MIL-HDBK-217 make use of mathematical expressions that predict failure rates of different electronic devices, according to parameters like temperature, voltage and environment. Although, several engineers with field experience have compared the experimental results to the standard and do not agree with the application of this standard to perform reliability predictions.

2.2. Coaxial Connectors

The test and measurement of critical parts are performed by coaxial connectors. Consequently, a study on the materials and manufacturing process are relevant to define high-level reliability.

The probability of a connector failure increases for reduced connector mechanical dimensions. Characteristics, such as concentricity, withdrawal and insertion forces and centre contact retention are used to ensure that a reliable connection during mating is established. Concentricity is a dimensional measurement that defines how centred the pin and socket are compared to the connector housing (higher stresses occur for higher concentricity values). The insertion and withdrawal forces are sliding forces with opposite directions that define the physical contact between the centre contacts (higher force values mean lower socket apertures or increased concentricity). The electrical characterization of the connector is performed by a Vector Network Analyser (VNA) both in terms of performance and repeatability. Some common failures are excessive wear of centre contacts, dirty mating surfaces and misalignment [2].

The materials used in a connector influences its reliability and performance. The choice of each material must have in consideration the electrical conductivity, machinability and high resistance to wear for different number of cycles. For the centre contacts, the common alloys are copper-zinc or copper-beryllium followed by a plating (nickel used as an under plating metal) [5, 4]. The component that sustains the centre contacts is the bead. The bead is a dielectric material as near to air as possible and it must offer mechanical stability and minimization of electrical reflections. The usual material for the bead is polychlorotrifluoroethylene (PCTFE). Finally, the connector housing can be made of brass or stainless-steel. Stainless steel provides higher durability and a better corrosion resistance. The remaining parts (spring and screws) are usually made by the same material than the housing [10].

The electrical evaluation of coaxial connectors is performed based on different parameters, namely the insertion loss and return loss, using a VNA. The VNA generates a sinusoidal stimulus signal to the DUT and measures the response of the DUT to the signal. In this project the main metric that is used to characterize electrically the connectors are the scattering parameters (S-parameters). The S-parameters describe how a device alters voltage waves determining whether there is loss or gain through the DUT [19, 18].

The 1.85 mm coaxial connector was the connector choice to fulfills the range of frequencies (24-70 GHz) required. It was originally introduced by

HP and it is mechanically compatible with the 2.4 mm coaxial connector. Due to the need of a blind mating interconnection between the ATE PCB test fixture and the DUT on the ATE test cell, a custom 1.85 mm blind mating connector was developed and is shown in figure 2.

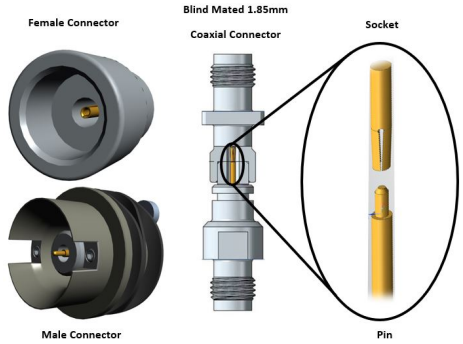

Figure 2: 3D models of the blind mating 1.85 mm coaxial connector designed for the Advantest V93000 ATE system.

The development and manufacturing of this connector was based on the MIL-PRF-39012 and IEEE 287 standard. These standards provide little guidance for the design,mechanical and electrical specifications and its testing for a blind mating interconnection. The materials and specifications for the custom designed 1.85 mm blind mating coaxial connector are shown in table 2.

Mechanical	
Insertion force	0.9 N
Withdrawal force	0.28 N
Contact durability	20,000 Cycles
Electrical	
Maximum Frequency	67 GHz
Impedance	50 Ω
Centre Conductor Resistance	3 mΩ Maximum
Environmental	
Temperature	0-55 °C
Materials	
Housing	303 Stainless Steel
Dielectric (Bead)	Neoflon ASTM D1430
Centre Conductor	BeCu C17300 TH04 [5]

Table 2: Target specifications and materials for the Blind Mating 1.85 mm Connector [21].

2.3. Reliability Engineering

The typical way to quantify it is through the use of mathematical statistical methods. The main goal of reliability engineering is to identify the causes of failure and correct them. Reliability is defined as the probability not to fail and is represented by expression 1 [17, 14].

$$R = e^{-\lambda t} \tag{1}$$

The function R(t) corresponds to the cumulative distribution function (CDF) and F(t) or unreliability function corresponds to the probability density function (PDF). Other typical factors associated with the study of reliability are the Mean Time to Failure (MTTF) and the failure rate ($\lambda(t)$). Each component has three periods of time that depend on the frequency of failure and failure cause pattern (represented by the bathtub curve in figure 3) [17, 14].

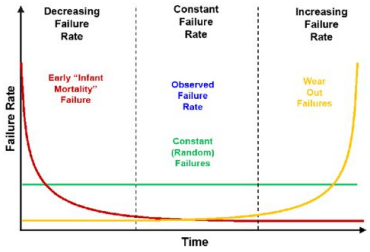

Figure 3: Bathtub curve with different reliability regimes.

2.3.1 Statistical Mathematical Methods

In reliability, statistical mathematical methods are used to infer properties of a large population from a smaller sample of data. The type of distribution used can be time or failure determined. The distributions considered along this project were weibull, lognormal and exponential.

When there are not many failure data, the statistical distributions make use of the Bernard approximation characterized by expression 2 which suggests that a minimum of 7 components are tested until failure.

$$F(t) = \frac{i - 0.3}{n + 0.4} \tag{2}$$

where $i = 1, 2, 3, 4$...Failed component and n is the total number of components tested [14].

Weibull is a two-parameter (β and η) distribution and it can be applied for any hazard rate values. The linear equation represented in expression 3 is obtained [17, 14].

$$lnln\left(\frac{1}{1 - F(t)}\right) = \beta ln(t) - \beta ln(\eta) \tag{3}$$

The lognormal distribution is applied for earlier failures in the life of devices. Examples of its use are in strengths of metals and dimensions of structural elements characterizing failures caused by fatigue. Similarly to weibull, it also depends on two parameters (σ and μ) and after applying a logarithm to the reliability function, expression 4 is obtained.

$$ln(t) = \mu + \sigma\Phi^{-1}F(t) \tag{4}$$

where a straight line is obtained by plotting the ln (t) in the y-axis and $\Phi^{-1}F(t)$ in the x-axis.

The exponential distribution is a particular case of the weibull distribution (when $\beta = 1$). It models time between two independent events that occur at a constant rate. Commonly used to describe the distribution of failure times of complex equipment. After the reliability function is linearized it results in expression 5.

$$ln\left(\frac{1}{1-F(t)}\right) = \lambda t \quad (5)$$

where the resultant points create a straight line that passes through the origin.

Table 3 summarizes the PDF correspondent for each distribution:

Weibull PDF	$f(t) = \left\{\frac{\beta}{\eta}\left(\frac{t}{\eta}\right)^{\beta-1} exp\left[-\left(\frac{t}{\eta}\right)^{\beta}\right]\right\}$	(6)
Lognormal PDF	$f(t) = \left[\frac{1}{t\sigma(2\pi))^{1/2)}} exp\left(\frac{-[ln(t)-ln(\mu)]^2}{2\sigma^2}\right)\right]$	(7)
Exponential PDF	$f(t) = \lambda e^{\lambda t}$	(8)

Table 3: PDF expressions used for the statistical distributions [17, 14].

2.3.2 Physics of Failure

The assessment of reliability is not only based on statistical methods, but also on Physics of Failure (PoF). This PoF analysis defines the failure mode, failure site and failure mechanism. The failure mechanisms can be due to mechanical, electrical or thermal conditions. Examples of material failure mechanisms are: creep, metal migration, corrosion, wear, fracture, fatigue or a combination of them. The SEM is an example of a methodology used to characterize the material failure mechanism. After identifying the failure mechanism, the correspondent statistical distribution is adjusted [17, 14].

Another way to investigate the failure mode analysis (FMA) is through the use of simulations, using the FEM. S-N (Stress vs number of cycles to failure) or Wöhler curves are utilized to express the fatigue strength of a material. This curve allows to predict the cycles to failure of a material based on the applied stress. Figure 4 represents a theoretical S-N curve [9].

Another important field of reliability testing, involves severe conditions of load, stress, voltage, temperature, humidity and others that in a normal operation it would not occur. This tests are performed to induce that a component fails earlier. The accelerated tests can be divided in thermal, chemical, electrical and mechanical stresses.

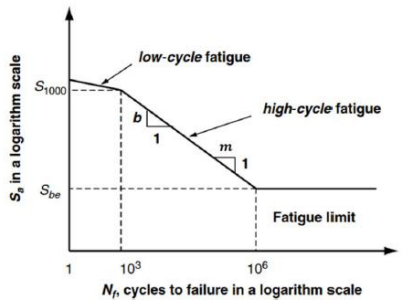

Figure 4: Generic S-N curve showing the different stages for a logarithmic scale.

2.3.3 Reliability of Coaxial Connectors

The connector reliability literature found can be separated in connectors for power applications and for high-frequency applications. In [24], silicon particles were added to simulate how the variations of contact resistance affected the contact failure. Weibull was the distribution adopted as a relationship between the concentration stress and characteristic life. In [23], SEM was used to do a metallurgical evaluation of the surface after an accelerated life test was applied. Before mating, the increase in contact resistance confirmed the presence of oxides. After mating, the measured contact resistance was lower due to the cleaning effect occurring on the surface. In [20] and [6] the focus is how the propagation of high-frequency signals affects the return loss (S12) and insertion loss (S11). In [20], nitric acid vapour was utilized to simulate a corrosion environment. The S-parameters were measured for a frequency range between 100 KHz and 3 GHz. The corroded surfaces increased the surface roughness over time and affected the electrical performance of the connector. Finally in [6], a total of 10,000 mating cycles were performed to study the repeatability of conenctor GPC-14, GPC-7, type N and SMA for a frequency range of 2 GHz and 18 GHz. The standard deviation is of less than 0.0082 dB. The main reasons of this variation is due to the stresses and strains introduced when 2 misaligned surfaces are forced to align. There are two reasons why the literature found cannot be applied to this work. First, because the connectors tested are for power applications or for frequency values lower than 18 GHz. Secondly, all coaxial connectors addressed are based on a threaded design which limits the application of a reliability model for blind mating coaxial connectors.

3. Testing Setup

The number of cycles chosen for each connector was 60,000. A total of 14 new connectors were tested. These values were a compromise between the available time to obtain the results and the required lifetime of a connector in an ATE system (5

insertions per day correspond to at least 10 years of usage).

From the 14 tested connectors, 12 were used to measure the electrical performance through S-parameters using a VNA. Two of those 12 connectors are subjected to an accelerated testing (85 ºC, 85 % humidity during 72 hours), defined by the JESD22-101, before the cyclic stress testing [25]. The remaining two of the 14 connectors were used to measure the electrical contact resistance using a multimeter.

The S-parameters were extracted from the VNA every 300 cycles and every 6,000 cycles the connectors were removed from the setup to perform mechanical and dimensional measurements. The total testing time for the 14 connectors was 3 months.

The S-parameters measurements were performed using a VNA without calibration. The reason for this is associated with the fact that in this study the goal is to obtain the difference between measurements for different number of cycles. Therefore, the measurement cable loss was not removed from the obtained measurement results. The advantage is that no re-calibration is required during the cyclic testing time.

Regarding the setup (shown in figure 5), matlab was the software used to implement an automated setup that allowed to control the docking and undocking of the ATE system through GPIB. The mechanical measurements were performed every 6,000 cycles using another setup, where a dial gauge measured the travelled distance of the insertion pins. The travelled distance must be of 1.3 mm (defined by the connector design) and the insertion pins geometry and materials are defined by the IEEE 287 standard.

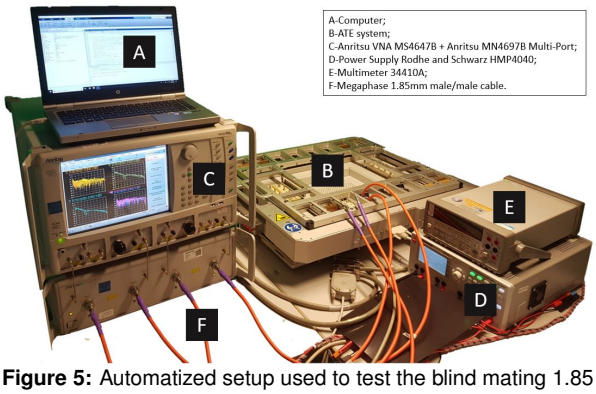

Figure 5: Automatized setup used to test the blind mating 1.85 mm connectors.

4. Testing results

The results herein are separated in electrical measurements (S-parameters and contact resistance), mechanical measurements (insertion and withdrawal forces) and dimensional measurements (concentricity and pin depth).

The S-parameters characterize either the connector has failed or not. The repeatability of S12 measurement is the criteria defined as the limit of a failed connector. This threshold must be lower than 2 dB, which includes temperature variations and cable movement. Figure 6 represents the S12 measurement for the failed connector number 5. The failure was identified at cycle 54,000 resulting in a resonant frequency of 20.6 GHz.

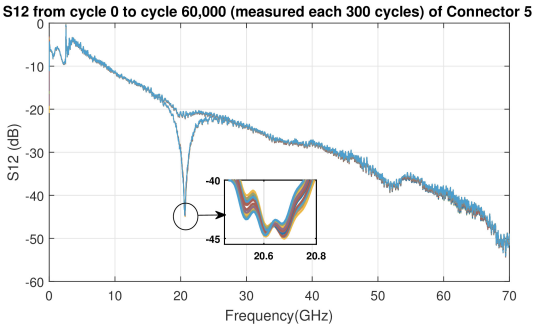

Figure 6: S12 measured for connector 5 in intervals of 300 cycles until 60,000 cycles.

In the case of connector 12, that has gone through an ACT before cyclic testing, it represented an earlier failure at cycle 24,900 with a resonant frequency of 8 GHz. Therefore, the ACT has influenced the lifetime of the connector. This means that for applications where the connector is subjected to higher humidity and temperature levels the reliability is affected by a factor of 2. Figure 7 shows a 3D plot of the variation of S12 measurements between 24,900 and 30,000 insertions. The first failure was registered at 24,900 cycle, although at cycle 27,3000 there is no resonance. This suggests that this connector presented an intermittent failure phenomena.

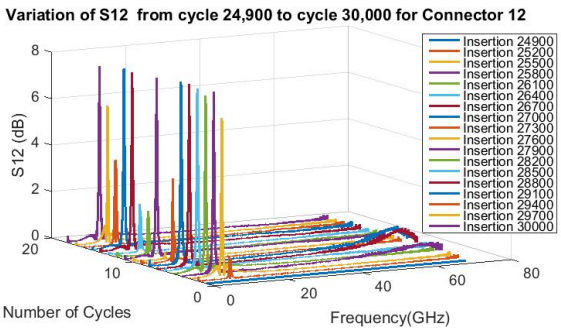

Figure 7: 3D plot that demonstrate the variation of S12 for the different number of cycles.

The S-parameters were measured before and after testing to account for the absolute performance of the connectors. This was performed using a 2-port VNA with calibration. Figure 8 represents the S12 measurement for connector 11.

The performance was practically not affected after 30,000 cycles. The highest variation is of 0.2 dB at higher frequencies.

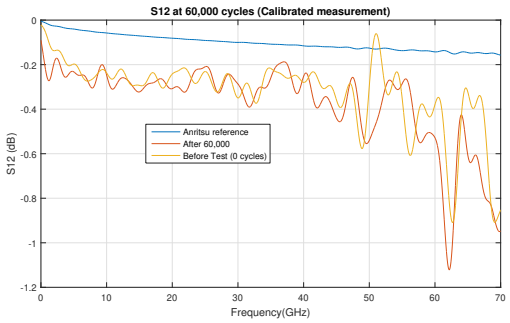

Figure 8: S12 performance of connector 11.

Connector 14 was tested to measure the contact resistance along 60,000 cycles to study their behaviour in other areas such as high-speed digital applications. The contact resistance is dependent on the area of contact between the socket and the pin. The failure is justified by the exponential increase after 48,000 cycles represented in figure 9. This is due to the presence of a crack at the keyhole of the socket. In practice, only one of the fingers of the socket is in contact with the pin. This results in a lower area of contact and therefore an increase of contact resistance.

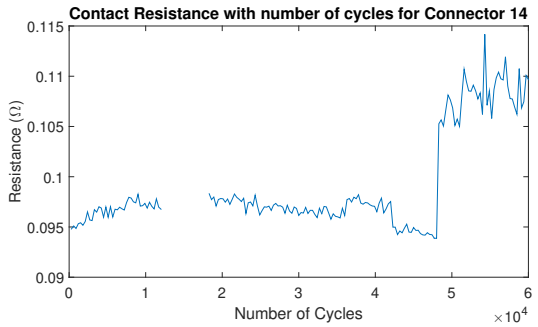

Figure 9: Contact resistance versus number of cycles for connector 14.

The withdrawal and insertion forces were the mechanical measurements performed. The results shown in figure 10 are only valid after 12,000 cycles since the correct insertion pins (made according IEEE 287 standard) were only used after that cycle. The difference of the values obtained experimentally compared to IEEE 287, is justified by the different design and connector manufacturing technology. Additionally, the instruments used to measure the forces were also different and the setup used may have induced misalignment which strongly influences the resultant value of forces.

The insertion and withdrawal forces decrease with the increasing number of insertions. When the values are close to zero there is no contact between the socket and the pin. At this point,

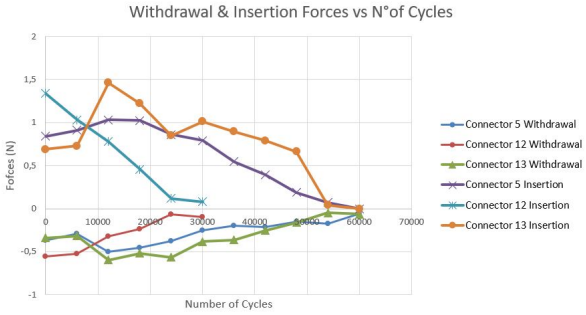

Figure 10: Withdrawal and insertion forces of connectors 5, 12 and 13, at different number of cycles.

the measured S-parameters present a resonance in the frequency spectrum and therefore the connector has failed. For a higher number of insertions, another factor that influences the value of the forces measured is the docking depth.

Concentricity measurements are not specified in any standard. This is a measurement that was defined by the connector designer to address the reliability of the connector. The acceptable value defined was 50 μm for the pin and socket. Figure 11 show the variation of concentricity as the number of cycles increase.

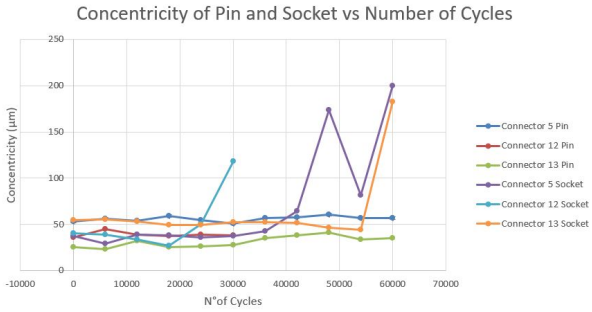

Figure 11: Concentricity of the pin and socket as a function of the number of cycles for connector 5, 12 and 13.

The pin concentricity was not affected with the increasing number of insertions. On the other hand, the socket concentricity was greatly affected when a failure occurs. Connector 5, 12 and 13 show an exponential increase for specific cycles that corresponds to the correspondent cycle where the connectors have failed.

After the measurements performed and on the connectors tested, reliability models were created based on statistical distributions such as weibull, lognormal and exponential. From the 14 tested connectors, only 7 were used to address the reliability models since there were some connectors that encountered setup problems and others were tested under different testing conditions. Based on the respective equations that characterize the different distributions (3, 4 and 5), the first step is to linearize the CDF function. Afterwards, based on

the reliability expressions, a plot of the probability of not to fail (reliability) versus the number of cycles is obtained for the measured 1.85 mm blind mating coaxial connector.

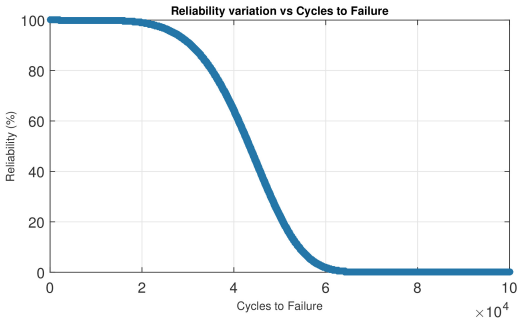

Figure 12: Reliability versus number of cycles for a 1.85 mm blind mating coaxial connector using a weibull distribution.

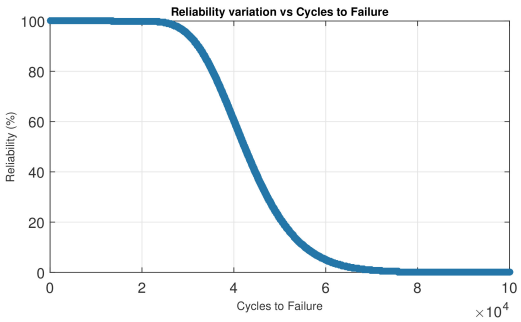

Figure 13: Reliability versus number of cycles for a 1.85 mm blind mating coaxial connector using a lognormal distribution.

Figure 12 and 13 show the reliability as a function of the number of cycles for lognormal and weibull distributions. Both distributions show that the reliability decreases mainly after 25,000 cyles. A limitation is the sample size which is not large enough to infer a reliability estimation for a higher population of connectors. Therefore, a future improvement would be to test a higher number of connectors.

5. Characterization

In order to do a characterization study in terms of PoF, the SEM and CT scan were the techniques utilized. Connector number 12 and 13 were the selected connectors to perform this characterization. The CT technique, used previously in medicine, has evolved into a powerful method for other industrial areas. The main components of a CT industrial machine are the X-ray tube, object manipulator and a detector. The CT equipment allows that several projections are obtained under different rotations for an object. The interaction of x-rays with different materials influence the contrast quality of the final object [8]. This technique does not require any sample preparation.

Figure 14 shows a scan of connector 12 after an ACT and after 30,000 insertions. The centre contacts do not have considerable degradation in terms of wear. Even though, the socket represents the highest deviation in one of the fingers (red region). This is related with the socket aperture. With the increasing number of cycles, the socket aperture increases mainly because the socket looses elasticity. The socket aperture can be accounted by the concentricity measurements or by measuring an angle α that represents how wide the fingers are.

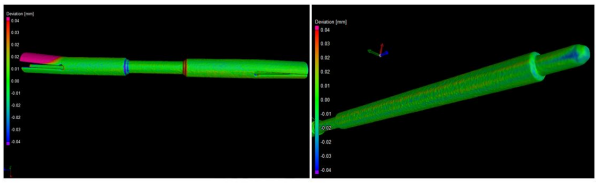

Figure 14: CT scan of the socket and pin of connector 12 after 30,000 cycles.

In order to identify the reason for the high values of socket aperture, figure 15 represents a scan performed only to the female connector. This scan shows a crack at the bottom of the socket. Therefore, the connector has failed due to a presence of a crack at the female pair.

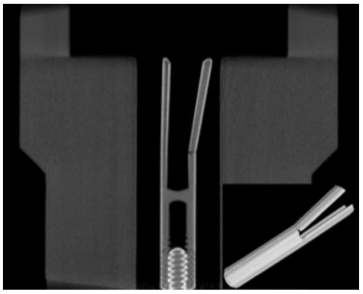

Figure 15: CT measurement of the crack of the female part of connector 13.

On the other hand, SEM is an ideal tool to obtain high-resolution images of small features. The centre contacts were analysed before and after testing. The goal is to measure the gold thickness and do an energy dispersive x-ray spectroscopy (EDS) analysis where the chemical elements are identified. From figure 16, we can conclude that the gold thickness is lower than the nickel thickness although both were within the range defined by the connector designer. The reason for this difference is related with the platting deposition difficulties present while plating an inner surface. From an EDS analysis, we can conclude that the ACT itself had no direct influence in terms of the gold and nickel layers and no other chemical elements were detected. Although, deepest grooves were present in connector 12, that has gone through 30,000 cycles, compared to connector 13 that was subjected to 60,000 cycles.

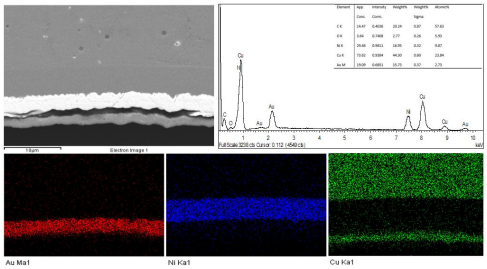

Figure 16: Representation of the thickness of the coatings applied and an EDS analysis performed to connector 12.

Figure 17 shows the inner fractured surface of connector 13 after removing out the tine/finger of the socket. Two different regions are identified. One zone shows the presence of a brittle fracture and the second one represents what appears to be striations. These striations are formed by localized plastic deformation occurring in the material and they are an evidence of fatigue. As the number of cycles increase, the micro cracks join together until the point that a macro crack is formed. At this point fracture occurs.

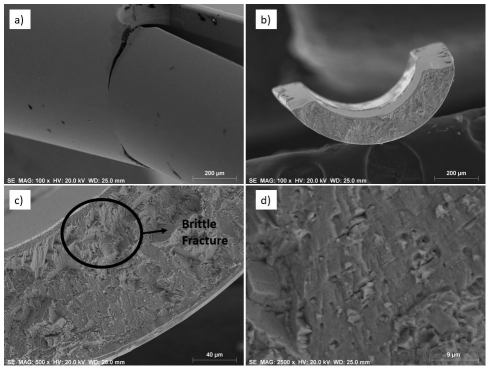

Figure 17: Analysis of fractured surface of connector 13. a) Crack appearance at the bottom of the socket; b) Picture of inside fractured surface after removing the finger from the socket; c) Picture of the brittle fracture; d) Amplification of the striations generated by fatigue.

The high number of insertions is directly related to fatigue, which is identified as the failure mechanism. Even though, the high stresses generated by the insertion pins while measuring the insertion and withdrawal forces had also influenced the lifetime of the connectors. Therefore, the failure mechanism is a combination of a brittle fracture with material fatigue.

6. Modelling

A FEM simulation was performed to the centre contacts. The main goals were to obtain the stresses and strains along the surface of contact. Two different simulations were accounted, one under elasticity conditions and the second under plasticity conditions. The software used to perform the mechanical simulations was COMSOL Multiphysics.

First, since the model is symmetric, the geometry is simplified to one fourth of the total model. Then, the material specifications are defined based on the C17300 TH04 [4] and added to COMSOL Multiphysics library. At this point, the physics of contact are established. The components were defined as a linear elastic material and the constraints and surfaces of contact are defined. The movement of the socket is defined by a prescribed displacement of 1.3 mm. This is achieved by using a periodic since (x) function, where x is the displacement.

In terms of meshing, the elements used were tetrahedral elements and the size is already predefined by COMSOL Multiphysics. Before running the simulation, a mesh convergence study was implemented to understand which was the best mesh. Different meshes were used to compare the results in terms of von Mises stresses shown in figure 18. To perform this study, a parametric sweep allowed to conclude that the best mesh is a fine mesh that compared to a finer mesh represents an error of 1.48 % (7 MPa difference).

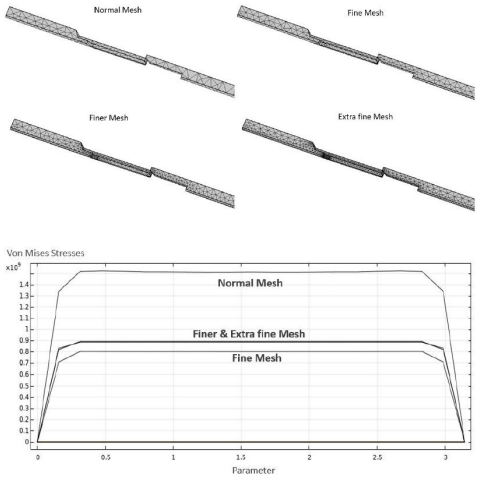

Figure 18: Study of mesh convergence using different meshes.

6.1. Simulation Results

For the first simulation, properties like the yield and ultimate strength and the elongation at break were not considered. As can be seen from figure 19, the highest stress occurs for a displacement of 0.92 mm and corresponds to 801.5 MPa. The highest values of stress occur at the keyhole of the socket.

The presence of strain in the three directions x,y and z allowed to conclude that the forces during contact exist for the different directions too. The values obtained for x, y and z direction are respectively 0.25, 0.08 and 0.4 N. Comparing to the 0.8 N experimental value, we can conclude that the vertical misalignment created by the force gauge may have influenced value of insertion and withdrawal forces. Consequently, a second simulation was executed where the pin was moved to a distance of

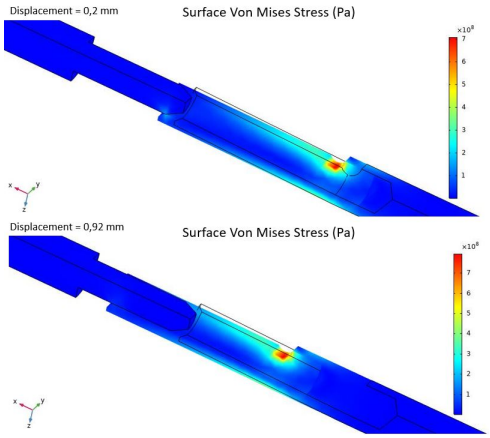

Figure 19: von Mises Stresses at different displacements assuming only the elasticity regime.

0.05 mm in the y and z directions to create a misalignment between the centre contacts. Figure 20 shows that the stresses are higher for a displacement of 1.3 mm. The maximum von Mises stress is of 4180 MPa which suggests that there is presence of plastic deformation.

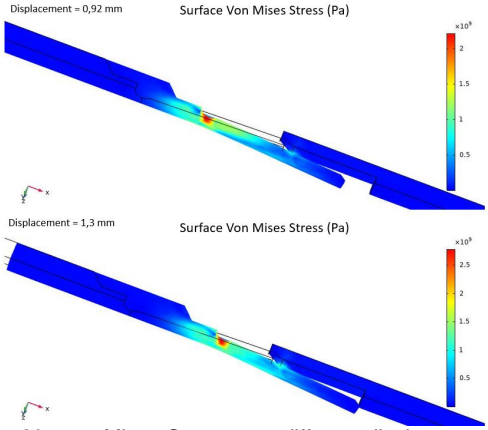

Figure 20: von Mises Stresses at different displacements assuming the plasticity regime.

Finally, based on the second simulation, the fatigue module allowed to calculate the cycles to failure. The S-N curves are used to address the HCF region and come as an input to the usage of the fatigue model by COMSOL Multiphysics. The S-N curve used in this case is based in the C17200 TH04 alloy [4], since any S-N curves were found for the C17300 TH04 alloy under study. The C17200 is the alloy that presents the closest mechanical properties to the C17300 alloy. Based on that, figure 21 represents the critical zones for the different insertions.

The minimum number of cycles to failure registered was 106,000. The disparity between this value and the experimental values (around 30,000 and 54,000 insertions) is related with the fact that the fatigue in this study is multiaxial. The S-N curve used, considered that the stresses occur in only one direction.

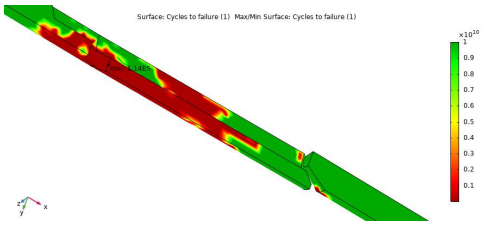

Figure 21: Cycles to failure obtained using the fatigue module used to obtain the cycles to failure.

7. Conclusions

The main goal of this work was to do a reliability study of a custom 1.85 mm blind mating coaxial connector. To do that, a reliability test plan was developed in collaboration with several engineers and companies. An automated setup was used with different measuring instruments controlled by matlab through GPIB.

From the 14 connectors, only three have survived. The earliest failure under ambient conditions was registered after 30,000 insertions. The ACT influenced the lifetime of the connectors and the earliest failure was registered at 24,900 cycles. The insertion and withdrawal forces decreased linearly as the number of cycles increase, and a minimum of 0.12 N for the insertion force was settled. The concentricity remained constant for the centre contacts before failure and increased exponentially for the failed connector sockets. The pin depth shows no valid relation to a failed connector. Weibull and lognormal distributions are considered as the valid reliability models, where assuming 99 % of reliability, 19,948 cyles to failure are obtained for weibull and 25,822 cycles to failure for lognormal.

The failure site was identified, by both CT and SEM techniques, at the female connector more specifically at the keyhole of the socket. The failed connectors represented a drop higher than 2 dB for the S12 measurement and an increase of the contact resistance measurements of 10 mΩ. CT scans evidenced diminished wear of the connector housing. A SEM analysis performed to the fractured surface, indicated the presence of striations (implies presence of fatigue) and brittle fractures. Similarly to the characterization methods, the mechanical simulations confirmed that the critical area (higher stresses and strains) occurred at the keyhole of the socket. The minimum number of cycles to failure were 106,000 cycles.

Overall, considering that for an ATE application the minimum number of cycles is 20,000, the custom designed 1.85 mm blind mating coaxial connector demonstrated high reliability.

References

[1] Accton. The Emergence of 5G mmWave. https://www.accton.com/Technology-Brief/the-emergence-of-5g-mmwave/ (accessed December 30, 2019).

[2] A. C. Charles Tumbaga. 0.8 mm Connectors Enable D-Band Coaxial Measurements, March 2019. https://www.microwavejournal.com/articles/31899-8-mm-connectors-enable-d-band-coaxial-measurements?v=preview (accessed December 30, 2019).

[3] J. Davies. Anticipating And Addressing 5G Testing Challenges, 2019. https://semiengineering.com/anticipating-and-addressing-5g-testing-challenges/ (accessed December 30, 2019).

[4] J. R. Davis et al. *Copper and copper alloys*. ASM international, 2001.

[5] J. Harkness, W. Spiegelberg, and W. Cribb. Guide to beryllium copper. 1988.

[6] R. Ji, J. Gao, G. Xie, G. T. Flowers, and Q. Jin. The impact of coaxial connector failures on high frequency signal transmission. In *2015 IEEE 61st Holm Conference on Electrical Contacts (Holm)*, pages 298–303. IEEE, 2015.

[7] J. Kelly. *Advanced production testing of RF, SoC, and SiP devices*. Artech House, 2006.

[8] R. Kramme, K.-P. Hoffmann, and R. S. Pozos. *Springer handbook of medical technology*. Springer Science & Business Media, 2011.

[9] Y.-L. Lee, M. E. Barkey, and H.-T. Kang. *Metal fatigue analysis handbook: practical problem-solving techniques for computer-aided engineering*. Elsevier, 2011.

[10] M. Maury Jr. Microwave coaxial connector technology: a continuing evolution. *Maury Microwave Corporation*, pages 1–21, 2005.

[11] D. McReynolds. Optimize Your RF/MW Coaxial Connections. https://www.rfindustries.com/resources/white-papers/optimize-rf-microwave-coaxial-connections.php (accessed December 30, 2019).

[12] P. Mhaisekar. An Incisive, In-depth Analysis on the 5g Tester Market, 2019. https://www.futuremarketinsights.com/reports/5g-tester-market (accessed December 30, 2019).

[13] J. Mundy. What is WiGig? https://5g.co.uk/guides/what-is-wigig/ (accessed December 30, 2019).

[14] D. Natarajan. *Reliable Design of Electronic Equipment*. Springer, 2015.

[15] Y. Nishi and R. Doering. *Handbook of semiconductor manufacturing technology*. CRC Press, 2007.

[16] D. of Defense. "MIL-PRF-39012, Connectors, Coaxial, Radio Frequency, General Specification for", April 2005. Retrieved 13 April 2012.

[17] M. Ohring. *Reliability and failure of electronic materials and devices*. Elsevier, 1998.

[18] D. T. Phillips and A. Garcia-Diaz. *Fundamentals of network analysis*, volume 198. Prentice-Hall Englewood Cliffs, 1981.

[19] T. S. Rappaport, R. W. Heath Jr, R. C. Daniels, and J. N. Murdock. *Millimeter wave wireless communications*. Pearson Education, 2014.

[20] Y. Ren, Q. Feng, T. Ye, and B. Sun. A novel model of reliability assessment for circular electrical connectors. *IEEE Transactions on Components, Packaging and Manufacturing Technology*, 5(6):755–761, 2015.

[21] B. Rosas. *AM70F70-101 and AF70F70-102 Connector Series Specifications*. Signal Microwave, April 2019.

[22] G. Subcommittee. Ieee standard for precision coaxial connectors. *IEEE Trans. Instrum. Meas*, 17(3):204–204, 1968.

[23] P. Varde, M. Agarwal, P. Marathe, U. Mohapatra, R. Sharma, and V. Naikan. Reliability and life prediction for electronic connectors for control applications. In *2010 2nd International Conference on Reliability, Safety and Hazard-Risk-Based Technologies and Physics-of-Failure Methods (ICRESH)*, pages 63–67. IEEE, 2010.

[24] Y. Zhou, Y. Su, Q. Li, Q. Jin, and J. Gao. A new lifetime prediction method based on particulate contaminants for coaxial connectors. In *2016 International Conference on Applied Mathematics, Simulation and Modelling*. Atlantis Press, 2016.

[25] C. Zorn and N. Kaminski. Acceleration of temperature humidity bias (thb) testing on igbt modules by high bias levels. In *2015 IEEE 27th International Symposium on Power Semiconductor Devices & IC's (ISPSD)*, pages 385–388. IEEE, 2015.